Carbohydrate Polymers 76 (2009) 622–631

Contents lists available at ScienceDirect

Carbohydrate Polymers

journal homepage: www.elsevier.com/locate/carbpol

Sorption behavior of ^{60}Co and $^{152+154}Eu$ radionuclides onto chitosan derivatives

E. Metwally [a], S.S. Elkholy [b], H.A.M. Salem [b], M.Z. Elsabee [b,*]

[a] Nuclear Chemistry Department, Hot Labs Center, Atomic Energy Authority, Cairo, Egypt
[b] Chemistry Department, Faculty of Science, Cairo University, Giza 11351, Egypt

ARTICLE INFO

Article history:
Received 2 November 2008
Received in revised form 13 November 2008
Accepted 18 November 2008
Available online 6 December 2008

Keywords:
Chitosan benzoyl thiourea
Radionuclides
Adsorption isotherms

ABSTRACT

Chitosan benzoyl thiourea derivative has been synthesized and used successfully for the removal of the hazardous ^{60}Co and $^{152+154}Eu$ radionuclides from aqueous solutions. Different parameters were applied for studying the adsorbitivity of these radionuclides, including change in pH, time, ion concentration, and equilibrium concentration. Freundlich and Langmuir isotherms were applied successfully to fit the experimental data. Two more isotherm models, Lagergren and Morris–Webber, have been applied. All the parameters and the constants calculated for the kinetic isotherms and models are evaluated and listed. A mechanism for the complex formation of Co^{+2} with the chitosan derivative has been suggested.

1. Introduction

Native chitin, poly-β-2-acetamide-(2-deoxy-D-glucopyranose) is the most important organic nitrogen containing polymer found in the oceans (McCarthy, Pratum, Hedges, & Benner, 1997) and the second most abundant material of the planet, being superimposed only by cellulose Subhash & Natarajan, 2000). Chitosan, poly-β-2-amino-(2-deoxy-D-glucopyranose), biopolymers is produced from the alkaline deacetylation of chitin. (Knaul et al., 1998). Thus, chitin as extracted from natural sources contains around 10% of free amino groups, while chitin submitted to an alkaline chemical reaction yields chitosan when the amino group units exceed 50% (Muzzarelli, 1973; Rhazi et al., 2002). The free amino groups distributed on the chitosan polymeric chain are effectively active in a series of chemical modifications (Abdou, Nagy, & Elsabee, 2008; Kurita, Mori, Nixhiyama, & Harata, 2002).

Chitin and chitosan, both are biocompatible biopolymers with low toxicities and significant biomedical applications (Khanal et al., 2001; Wang, Kao, & Hsieh, 2003). An expressive chitosan application is associated with its ability to extract cations from aqueous solution, due to the availability of the free amino groups. Thus, this biopolymer can be potentially used as an extractor support to remove undesirable cations from an ecosystem (Mitani, Moriyama, & Ishi, 1992).

There are numerous reports concerning the adsorption of metal ions onto chitosan (Blazquez, Vicente, Gallo, Ortiz, & Irabien, 1987; Muzzarelli, Raith, &, Tubertini 1970; Muzzarelli &, Rocchetti, 1974; Muzzarelli, & Sipos, 1971; Onsoyen & Skaugrad, 1990; Sakaguchi, Horikoshi, & Nakajima, 1981). The presence of hydroxyl and amine groups can serve as chelating sites and can be chemically modified into chitosan derivatives with high adsorption capacity for ionic species (Chu, 2002; Evans, Davids, MacRae, & Amirbahman, 2002; Guibal, 2004; Juang & Shao, 2002; Wu, Tsengm, & Juang, 2000). Introducing sulfur in chitosan produces material with better antibacterial properties and higher sorption capacity for metal ions from solutions (Chen, Wu, & Zeng, 2005; Guibal, Vincent, & Mendoza, 2000; Kumar, Muzzarelli, Muzzarelli, Sashiwa, & Domb, 2004), the latter work initiated our interest to prepare similar thiourea derivatives for chitosan used in the present work (Peter, 1995).

Adsorption and determination of metal ions such as zinc (II) and vanadium (II) onto chitosan from sea water have been studied (Muzzarelli & Rocchetti, 1974; Muzzarelli & Sipos, 1971; Muzzarelli et al., 1970). Adsorption of strontium (II), cobalt (II), zinc (II) and iron (III) on chitosan from a sodium chloride solution have been reported (Nishimura, Imai, & Watari, 1995). Adsorption behavior of Cu (II) (Minamisawa, Jigiri, Arai, & Okutani, 1996; Wu et al., 2000) and cobalt (II) (Minamisawa, Iwanamia, Arai, & Okutani, 1999) were investigated. Chitosan from different sources was used in the form of beads and flakes and the adsorption capacity for Cu (II) was almost unaffected by the physical form of the polymer while dye adsorption was much higher on beads than on the flakes. Langmuir isotherm was found to fit the adsorption process (Wu et al., 2000). Chitosan and some of its derivatives have been used effectively for the adsorption of mercury (II) (Babel & Kurniawan, 2003; Cardenas, Orlando, & Edelio, 2001). Radiation crosslinked chitosan has been used recently for the adsorption of Cr (VI) from aqueous media and its application for the treatment of wastewater contaminated with Cr (VI) (Ramnani & Sabharwal, 2006).

Adsorption of numerous heavy and hazardous metal ions by chitosan have been investigated by many authors (Benavente, Arévalo, & Martínez, 2006; Igwe, Ogunewe, & Abia, 2005; Minamisawa,

* Corresponding author. Tel.: +20 26352316.
E-mail address: mzelsabee@yahoo.com (M.Z. Elsabee).

0144-8617/$ - see front matter © 2008 Elsevier Ltd. All rights reserved.
doi:10.1016/j.carbpol.2008.11.032

Minamisawa, Yoshida, & Takai, 2004; Rojas et al., 2005; Su, Wang, & Tan, 2003; Wan Ngah, Kamari, & Fatinathan, 2006).

Much less work had been devoted for the application of chitosan and its derivatives for the absorption of radioactive elements. In the present study sorption behavior of ^{60}Co and $^{152+154}$Eu radionuclides onto chitosan derivative is presented. The selection of ^{60}Co and $^{152+154}$Eu was due to their importance as fission product radionuclides and their presence in low level radioactive wastes produced from different researches activities. Chitosan with thiourea moiety has been chosen in anticipation for a higher adsorption power. Kinetic approach for the adsorption of both isotopes is determined using different isotherms. Freundlich, Langmuir, Lagergren, Reichenberg and Morris–Webber isotherms are applied for the resulting adsorption data.

2. Experimental

2.1. Chemicals and reagents

All the reagents used were of AR grade chemicals. Chloride salts of cobalt and europium were purchased from the Amersham Radiochemical Center.

2.2. Preparation of chitosan benzoyl thiourea derivative CTU

The thio derivative used in this work has been prepared according to reference (Eweis, Elkholy, & Elsabee, 2006) and is illustrated in Scheme 1.

All samples were extracted in soxhlet for 6–8 h with acetonitrile and ethanol to remove the unreacted isothiocyanate, dried in oven at 60 °C until constant weight.

Different derivatives with various benzoyl isothiocyanate: chitosan ratios have been prepared and were assigned as 1B, 2B, 3B, 4B and 5B for the ratios 0.5, 1, 2, 3 and 5, respectively. The derivatives with the higher ratios (excess isothiocyanate) may have substitution in the OH group as well.

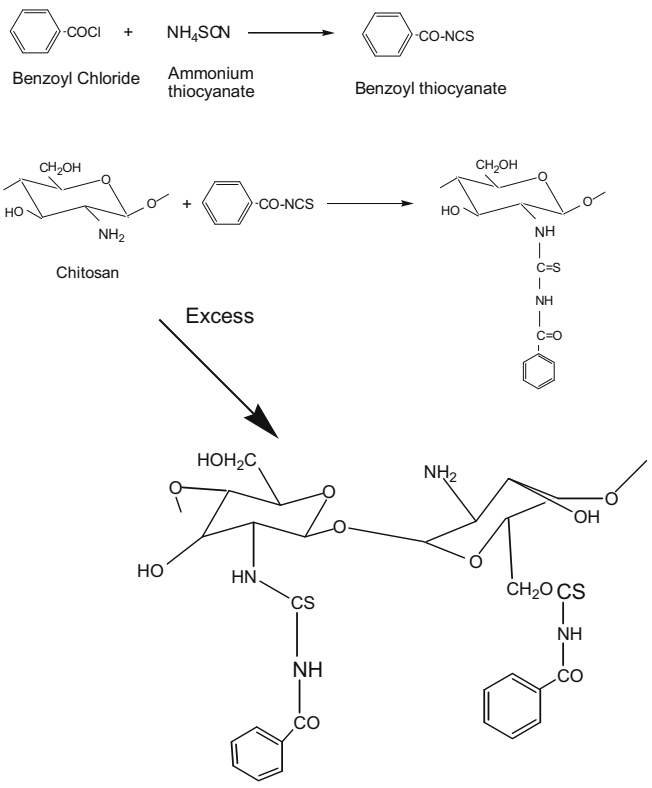

Scheme 1. Preparation of chitosan benzoyl thiourea. Two possible sites for the reaction of benzoyl isothiocyanate with chitosan.

The type of derivative used mainly in the present study is 2B. The pale yellow polymer was sieved using a sieve with mesh size of 370 μm and particle size diameter of <370 μm and was used for all experiments.

2.3. Characterization of the CTU (2B)

2.3.1. FTIR spectroscopy

FTIR spectra were taken using FTIR spectrometer Bruker Vector 22 Germany in the range of 400–4000 cm^{-1}.

2.3.2. Elemental analysis

Elemental analysis was conducted in the Microanalytical unit in Cairo University for (1B, %) C = 40.02, H = 6.4, N = 8.43 and S = 4.74, (2B) C = 45.24, H = 5.57, N = 8.32, S = 7.24, (3B) C = 40.8, H = 6.32, N = 8.6, and S = 5.46, (4B) C = 39.25, H = 6.04, N = 9.58, S = 8.68 and for (5B) was C = 41.12, H = 6.06, N = 9.40 and S = 7.60. The elemental analysis shows the increased extent of substitution with increasing the isothiocyanate:chitosan ratio as expected, all the CTU derivatives are insoluble so it was not feasible to measure their ^{1}HNMR spectra.

2.3.3. X-ray diffraction analysis

X-ray diffraction measurements were carried out using Scintag/USA XGEN-4000 at 45 kV and 40 mA using Ni-filtered Cu K_α radiation. A measure of the crystallinity was obtained by comparing the area of the crystallinity peaks to the whole area.

2.4. Radiometric assay

^{60}Co and $^{152+154}$Eu isotopes were produced by neutron irradiating an appropriate weight of their corresponding salts in Inshas second reactor ERR-2. Aqueous solutions of cobalt and europium were prepared by dissolving a known quantity of both cobalt (II) chloride and europium (III) chloride, respectively, in double-distilled water, which was labeled with ^{60}Co and $^{153+153}$Eu isotopes and kept as stock radioactive solutions for further use. The activity of ^{60}Co and $^{152+154}$Eu isotopes in aqueous solutions was measured using NI scintillation detector connected to Nucleus gamma counter.

2.5. Adsorption technique

Batch technique was applied to investigate the different parametric effects on the sorption process. Where a certain weight 0.05 g (m) of the CTU was mixed with a certain volume 5 ml (V) of ^{60}Co or $^{152+154}$Eu aqueous solutions and equilibrated by shaking in a shaker with speed 300 rpm at room temperature. The ratio of V/m was kept constant for all the experiments. The solutions were separated after a certain time and the concentration of each ion was determined radiometrically. The adsorption coefficient and the uptake% of the element between the aqueous phase and the ion exchanger were determined using the following equations:

$$k_d = \left(\frac{(A_i - A_f)}{A_f}\right) x \frac{V}{m} \quad (1)$$

$$\text{Uptake}\% = ((A_i - A_f)/A_i) \times 100 \quad (2)$$

Where, K_d, is the adsorption coefficient. A_i, is the area under the gamma energy peak for the corresponding isotope before contact-

ing the ion exchanger. A_f, is the area under the same peak for the corresponding radioisotope after contacting the ion exchanger.

2.6. Kinetic and sorption isotherms

The kinetic behavior of Co^{2+} and Eu^{3+}ions on CTU was followed up by application of batch technique. Sorption isotherms for Co^{2+} and Eu^{3+} were determined over the concentration range of 10^{-5}–10^{-2} M from 0.02 M NaCl as electrolyte background solution. The amount of ions adsorbed onto chitosan, q_t (mg/g), was calculated by the following relationship (Metwally 2006; Ravindran, Steven, Badriyha, & Pirbazari, 1999; Schmuhl, Krieg, & Keizer, 2001):

$$q_t = (C_o - C_t)(V/W) \quad (3)$$

Where, C_o and C_t are the initial and final concentrations at certain time t of the ions in the liquid-phase (mg/L), respectively. V, is the volume of the solution (L) and W is the weight of CTU used (g).

3. Results and discussion

The FTIR spectra of chitosan, CTU B2 sample and Co^{+2}-2B complex are shown in Fig. 1. The spectrum of chitosan shows the characteristic bands at 3424 cm^{-1} for the O—H and N—H stretching vibrations, the —CH_3 (of the residual acetamide group) at 2921 cm^{-1} and C—H at around 2876 cm^{-1}. The amide I band at 1654 cm^{-1} and at 1602 cm^{-1} (amide II) and pronounced bands at 1157.5, 1073.5 and 1031.5 cm^{-1} for the C—O—C and C—O stretching can be seen together with the in-plane O—H bend at 1379.6 cm^{-1}.(Fig. 1a). The spectrum of 2B sample (Fig. 1b) shows the following bands: ν_{max} (cm^{-1}) 3420.7 (N—H, O—H groups broad band) 3059, 2975 (C—H, —CH_2 and phenyl group), 1654.9, 1620.2, 1603.6, 1559, and 1525 cm^{-1}, in general when the C=S group is attached to a nitrogen atom the spectrum shows an absorption band in the general C=S stretching region (lower than the C=O band). In addition several other bands in the broad region of 1500–700 cm^{-1}

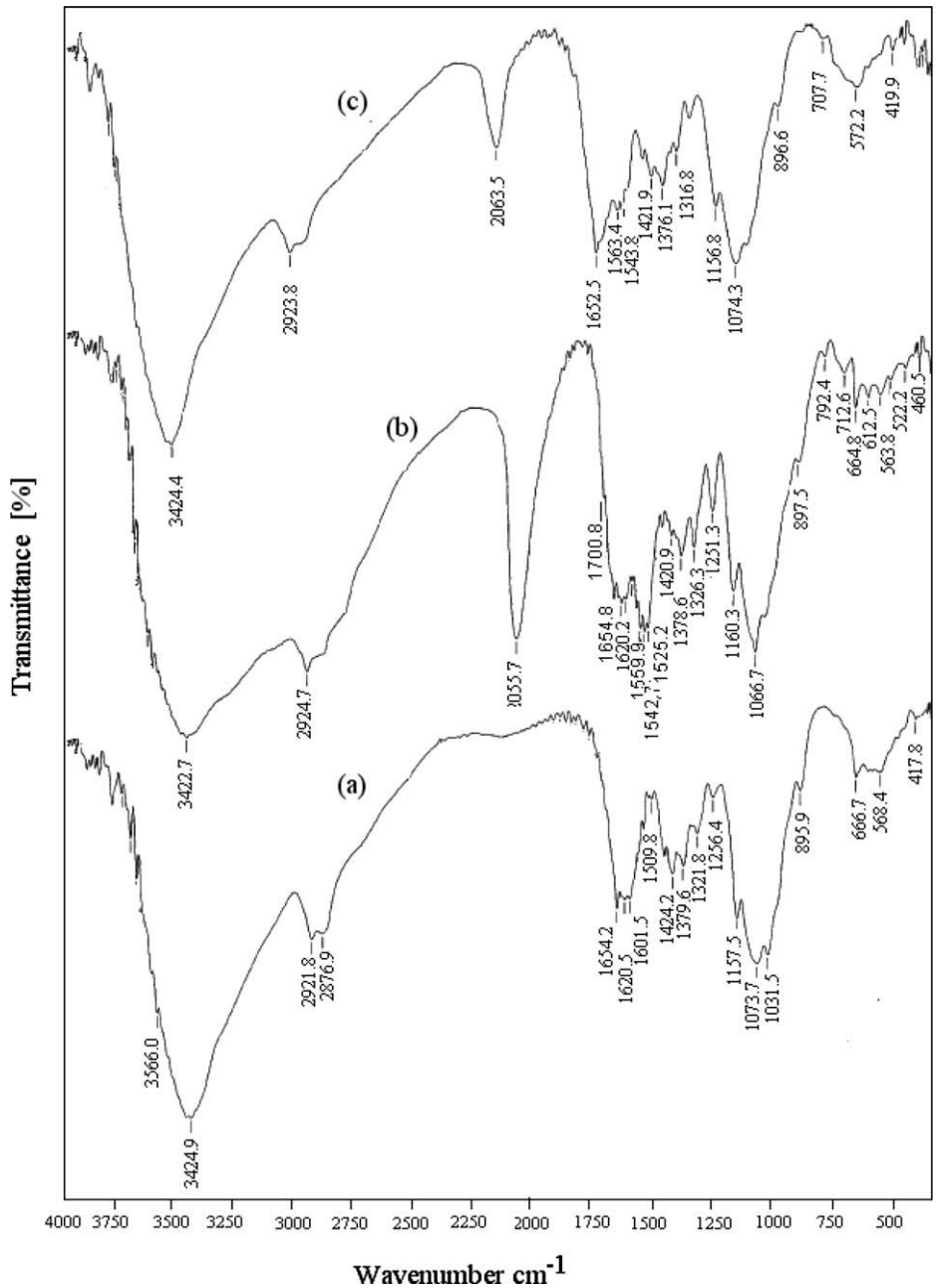

Fig. 1. FTIR spectra of (a) chitosan (b) CTU B2 (c) Co $^{+2}$-CTU (B2) complex.

can be attributed to the vibrations involving interaction between the C=S and the C—N stretching (Silverstein, Webster, & Kiembe, 2005).The most characteristic band however is the band at 2056 cm^{-1} which was not observed in pure chitosan. This band was present in all the CTU samples and was detected even after several hours' soxhlet extraction with acetonitrile followed by ethanol. This band may be due to the tautomeric structure:

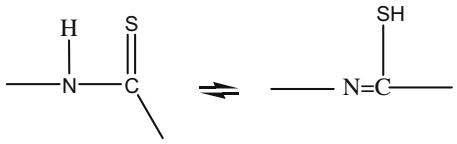

Also a shoulder at 1700 cm^{-1} indicative of a carbonyl group stretching vibration, the spectrum of the complex compound shows a similar pattern with differences in the region of 1650–1500 cm^{-1}, which could be attributed to the participation of both the C=O and C=S bonds in the chelation reaction. The intensity of the band at 2063 has been reduced and shifted slightly by about 8 cm^{-1} after complexation with Co^{+2} ions. The chelation process is currently being investigated in more detail in order to throw more light on the complexation process.

Fig. 2 illustrates X-ray diffraction diagrams for some CTU samples. The X-ray analysis was conducted to find out the effect of the chemical modification upon the percent crystallinity of the original chitosan. Two sharp peaks were found for sample 1B (lowest substitution %) at around 9° and 21° 2θ values. Percent crystallinity was found to be: 1B-43.93 3B = 35.65 and 5B = 33.73 indicating lowering of the crystallinity with increasing the extent of substitution reaction.

3.1. Influence of different types of CTU on ion adsorption

The uptake% of Eu(III) and its corresponding distribution coefficient values determined for the different derivatives are listed in Table 1. The recorded uptake% using 2B sample has the maximum value, 45.98%, for Eu(III) adsorption from aqueous solution of trace ion concentration at pH = 2.5.

Adsorption of Eu(III) onto the various CTU at different ion concentration in the range of 10^{-6}–10^{-3} M was determined and listed in Tables 1 and 2. It is observed that the uptake% of Eu(III) is higher in low ion concentration using 2B than using the 5B derivative. The same finding was observed at higher ion concentration.

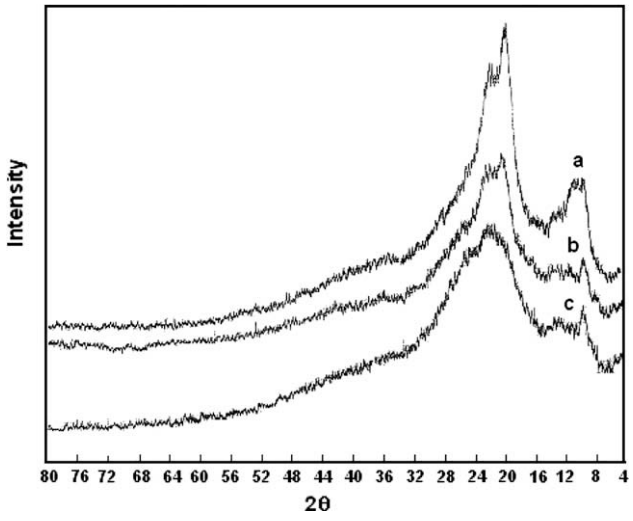

Fig. 2. X-ray diagrams for (a) 1B, (b) 3B and (c) 5B samples.

Table 1
Uptake% of Eu(III) on different types of CTU from aqueous solution at pH = 2.5 using trace ion concentration of $^{152+154}$Eu isotope.

Chitosan type	Uptake%	K_d	q_e (mg/g)
1B	44.92	81.55	6.82×10^{-3}
2B	45.98	85.51	6.98×10^{-3}
3B	39.14	64.43	5.94×10^{-3}
4B	35.2	57.94	5.3×10^{-3}
5B	32.9	49.08	4.9×10^{-3}

3.2. Effect of pH

Effect of pH on the adsorption of Co(II) and Eu(III) onto CTU (2B) was studied and presented in Fig. 3. Chitosan beads have been known to be unstable or start to swell in solution of lower pH. Therefore, the chitosan beads did not act as an adsorbent in lower pH region (pH 1–2) (Minamisawa et al., 1996). Uptake% of Eu(III) and Co(II) reaches its maximum values of 75.0% and 98.0% at pH 3.5 and 8.0, respectively, at 10^{-5} M ion concentration.

3.3. Complex formation

The mechanism of complex formation and structure of the formed complex in this case i.e. using CTU is still unclear and may require additional analytical tools (e.g. solid state NMR spectrometer) which could be available in the near future. However a proposed structure for the CTU/Co complex can be represented as in Scheme 2.

3.4. Sorption isotherm models

Investigations carried out on the rate of sorption for the studied ions onto CTU 2B from aqueous chloride solution indicated that the

Table 2
Freundlich and Langmuir parameters data for the sorption of Cobalt and Europium from aqueous chloride solutions by polymeric chitosan adsorbent.

Isotherm		Co(II)	Eu(III)
Type	Parameters		
Freundlich	K_F (mg/g)	14.140	33.682
	1/n	0.7451	0.94224
	R^2	0.99592	0.99998
Langmuir	Q^o	5.1055	13.2362
	b	52.8799	0.4511
	K_a	26.9978	5.9708
	R^2	0.98002	0.99168

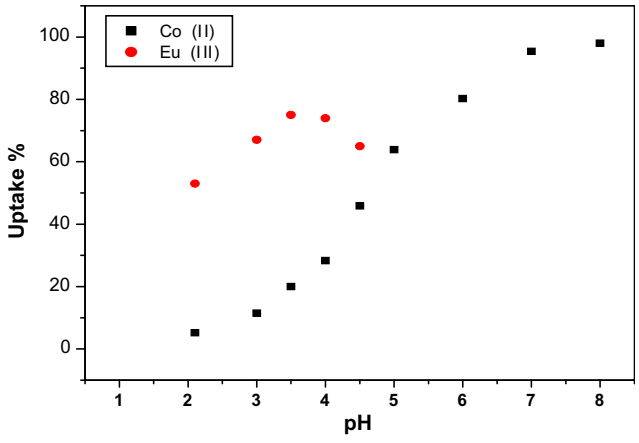

Fig. 3. Effect of pH on the adsorption of Co(II) and Eu(III) on CTU (2B).

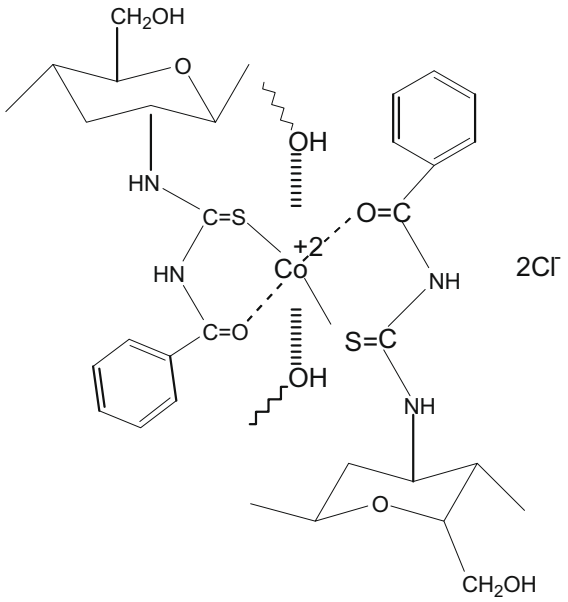

Scheme 2. Proposed mechanism for the absorption of Co^{+2} onto CTU.

amount adsorbed of cobalt reaches 3.53 mg/g after 1 h and 3.78 mg/g for europium after 4 h of contact time, respectively, at 10^{-3} M ion concentration. Also, their corresponding values resulted at 10^{-2} M ion concentration are 34.54 (mg/g) and 29.47 (mg/g), respectively. The data are presented in Fig. 4. Where, it is clear that 1 and 4 h are sufficient of contact time for the equilibration of Co(II) and Eu(III), respectively. The equilibrium adsorption of Co(II) and Eu(III) on CTU as a function of the equilibrium concentration of the studied ions are shown in Fig. 5. The isotherms obtained are regular, positive, and concave towards the concentration axis. The initial rapid sorption indicated a slow approach to equilibrium with higher metal ion concentrations.

Then there was a gradual increase in the sorption of both ions until an equilibrium was attained. An equilibrium concentration of Co(II) and Eu(III) ions was reached at about 5×10^{-3} M and 7.5×10^{-3} M, respectively at which the saturation capacity of adsorption for both ions is achieved as seen from Fig. 5. The distribution of the studied ions between the solid–liquid interface at equilibrium, has been treated with Freundlich and Langmuir isotherms.

Freundlich isotherm could be written as (Ravindran et al., 1999):

$$\log q_e = \log K_F + 1/n \log C_e \quad (4)$$

where q_e is the amount of the solute adsorbed per unit weight of the sorbent (mg/g), C_e is the equilibrium concentration of the solute in the bulk solution (mg/L), K_F is a constant points toward the relative sorption capacity of the sorbent (mg/g) and $1/n$ is a constant related to the intensity of the sorption processes. Freundlich isotherm plots of both the studied ions are presented in Fig. 6. The straight lines obtained indicate that sorption of Co(II) and Eu(III) fits with the Freundlich isotherm. Slopes of the Freundlich plots equal to 0.7451 and 0.9422 for Co(II) and Eu(III) ions respectively. The slope value (<1) indicates that the sorption of these ions onto the CTU biopolymer is a concentration-dependent process (Sheha & Metwally, 2007). This may be attributed to the fact that with progressive surface coverage of the adsorbent, the attractive forces between the metal ion species such as Van der Waals forces, increases more rapidly than

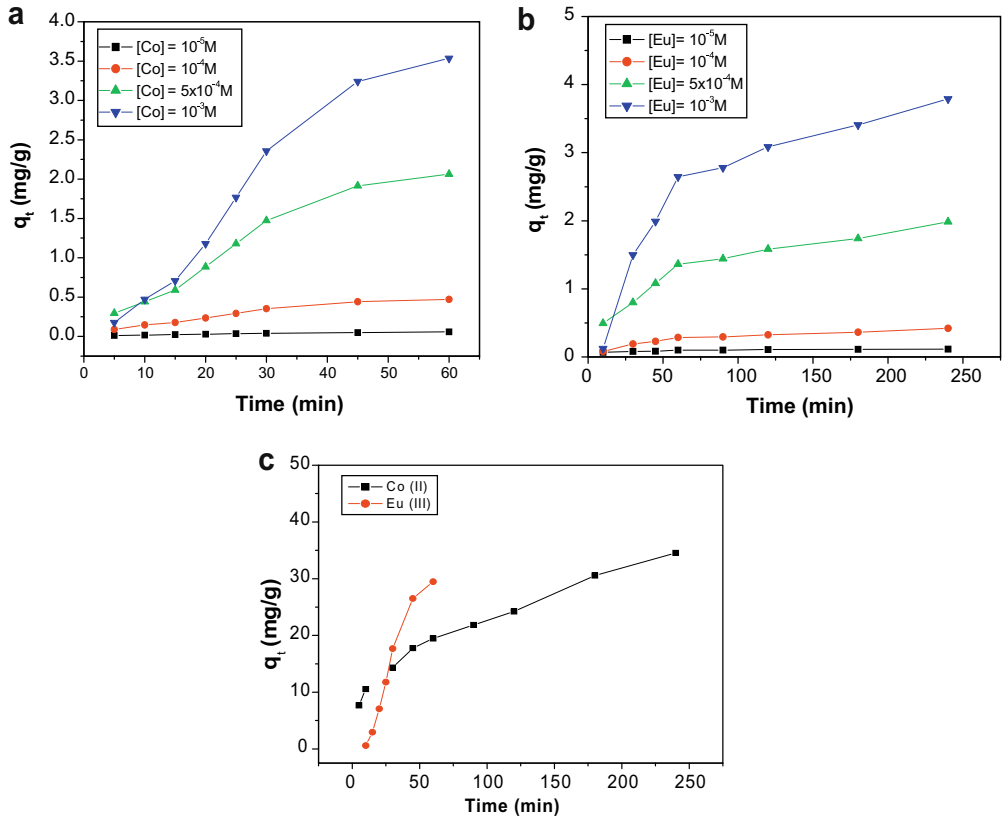

Fig. 4. The amounts adsorbed of the studied ions onto CTU (2B) with changes of time at different ion concentration. (a): Co(II), (b): Eu(III) and (c): for both ions at 10^{-2} M.

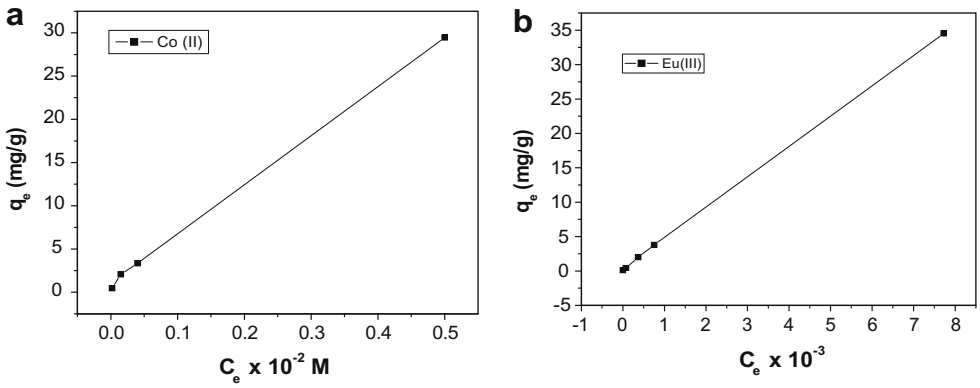

Fig. 5. Amount adsorbed of (a): Co(II) and (b): Eu(III) as a function of equilibrium ion concentration.

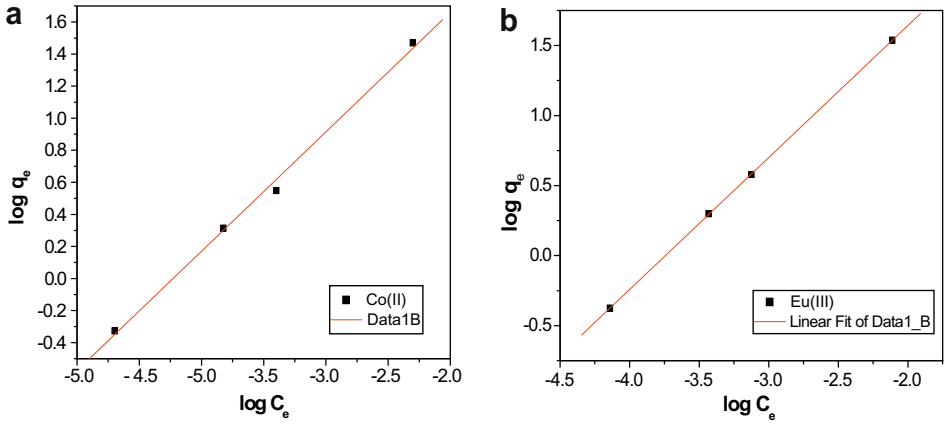

Fig. 6. Freundlich isotherm for the adsorption of (a): Co(II) and (b): Eu(III) onto CTU (2B).

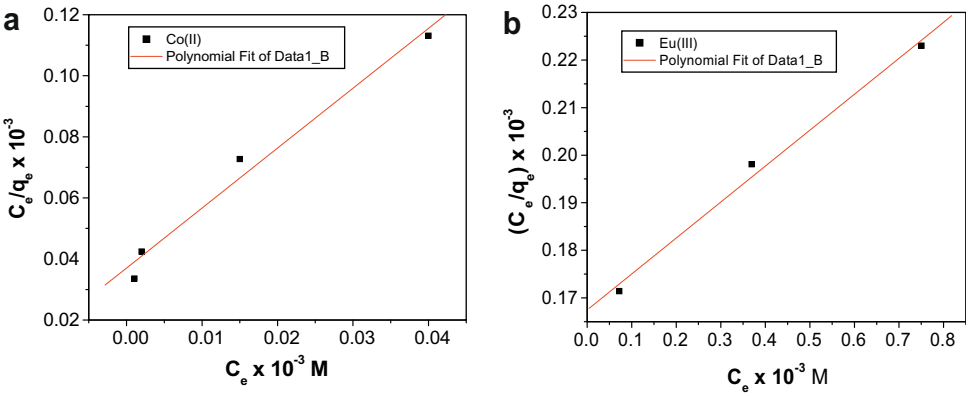

Fig. 7. Langmuir isotherm for the adsorption of (a): Co(II) and (b): Eu(III) onto CTU at 10^{-5} M ion concentration.

the repulsive forces, exemplified by short-range electronic or long-range coulombic dipole repulsion, and consequently, the metal ions manifest a stronger tendency to bind to the polymer surface (Ravindran et al., 1999).

The data obtained from the Freundlich isotherm suggest that the sorption processes could not be restricted for a specific class of sites and assume surface heterogeneity. Table 2 illustrates the Freundlich parameters calculated for the sorption of Co(II) and Eu(III) and the correlation coefficient values (R^2). for these ions.

Langmuir isotherm could be written as (Metwally, 2006):

$$C_e/q_e = (1/Q^o b) + (1/Q^o)C_e \quad (5)$$

Where, q_e is the amount of the ion adsorbed per unit weight of sorbent (mg/g), C_e is the equilibrium concentration of the solute in the bulk solution (mg/L), Q^o is the monolayer adsorption capacity (mg/g) and b is a constant related to the free energy of adsorption ($b \propto e^{-\Delta G/RT}$). The obtained data are presented in Figs. 6 and 7, and the corresponding Langmuir parameters for the adsorption of the studied ions are listed in Table 2. The monolayer adsorption capacity Q^o for the sorption of Eu(III) was higher than that for Co(II) ions. Since the overall rate constant k_a equals to the product of Langmuir parameters ($b \times Q^o$) (Ravindran et al., 1999). From the obtained data it is found that the overall rate constant k_a for cobalt is higher than that for europium ions.

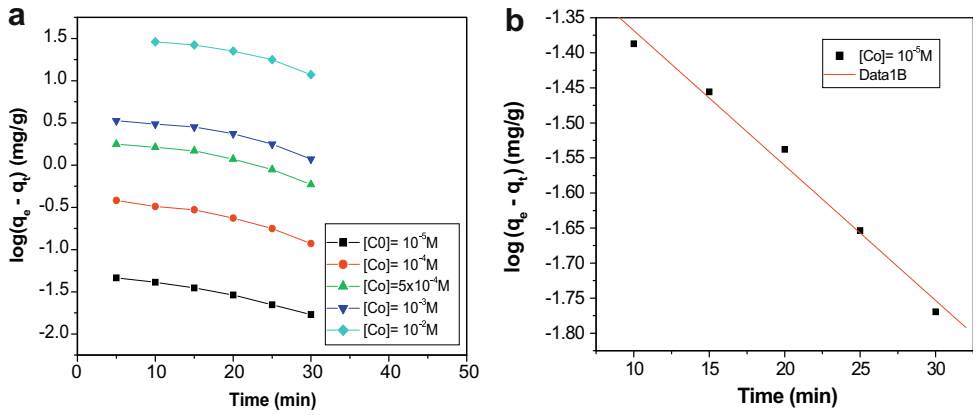

Fig. 8. (a) Lagergren kinetic isotherm for adsorption of Co(II) onto CTU (2B) at pH = 8, at different ion concentration (b) [Co] = 10^{-5} M showing linearity of the plot.

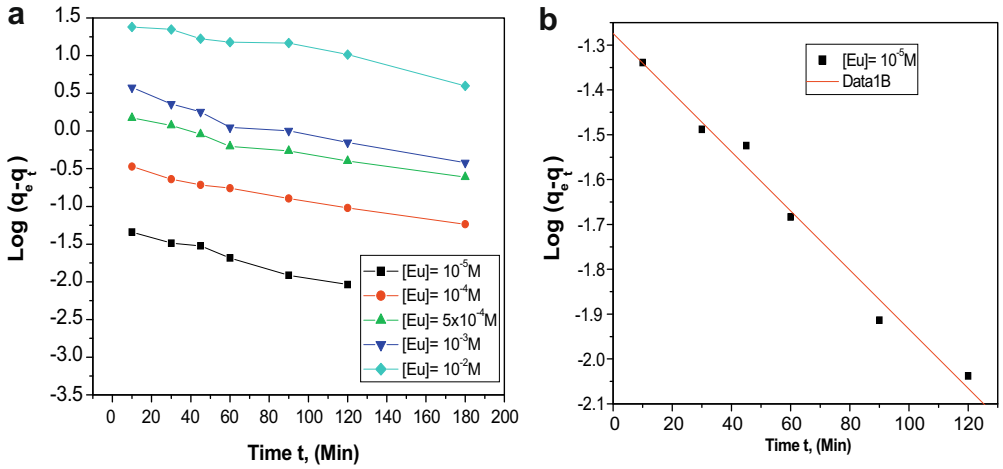

Fig. 9. Lagergren kinetic isotherm for adsorption of Eu(III) onto CTU (2B) at pH = 3.1, at different ion concentration. [Eu] = 10^{-5} M showing linearity of the plot.

3.5. Kinetic studies

The characteristics and the diffusion resistance of the surface of the sorbent play an important role in the rate of sorption and accordingly the overall transport of the solute. Therefore, the application of an appropriate kinetic model is important to determine and to shed light on the changes of sorption of the studied ions with time. In the present study two kinetic models have been applied and evaluated.

The first model used, is the first order Lagergren kinetic isotherm which could be written as (Justi, Fávere, Laranjeira, Neves, & Peralta, 2005):

$$\log\,(q_e - q_t) = -\log q_e - (kt/2.303) \qquad (6)$$

Where, q_e (mg/g) is the concentration of the ion adsorbed at equilibrium, q_t (mg/g) is the concentration of the ion adsorbed at time t, and k is the rate constant. It could be observed from Figs. 8a and 9 (8(b) and 9(b) are two examples to show the linearity of the Lagergren equation for just one concentration) that the sorption of Co(II) and, Eu(III) ions had followed the Lagergren equation over the entire period of investigation at different ion concentrations. The data in these figures were subjected to regression analysis and the values calculated for the first order rate constants from the slopes of the straight lines reported for the adsorption of Co(II) and Eu(III) are in the ranges 0.0212–0.0635 and 0.0099–0.0152, respectively. As listed in Table 3, there is no big variation for the overall rate constant values with the change of ion concentration.

Table 3
Lagergren parameters for the adsorption of Co(II) and Eu(III) onto CTU (B2) biopolymer from aqueous solution.

Lagergren isotherm	Co(II)					Eu(III)				
Parameters	Ion concentration, M					Ion concentration, M				
	10^{-5}	10^{-4}	5×10^{-4}	10^{-3}	10^{-2}	10^{-5}	10^{-4}	5×10^{-4}	10^{-3}	10^{-2}
k (min^{-1})	0.0443	0.0635	0.0607	0.0212	0.0574	0.0152	0.0099	0.0099	0.0127	0.0100
R^2	0.9868	0.9899	0.9820	0.9602	0.9797	0.992	0.991	0.991	0.973	0.970

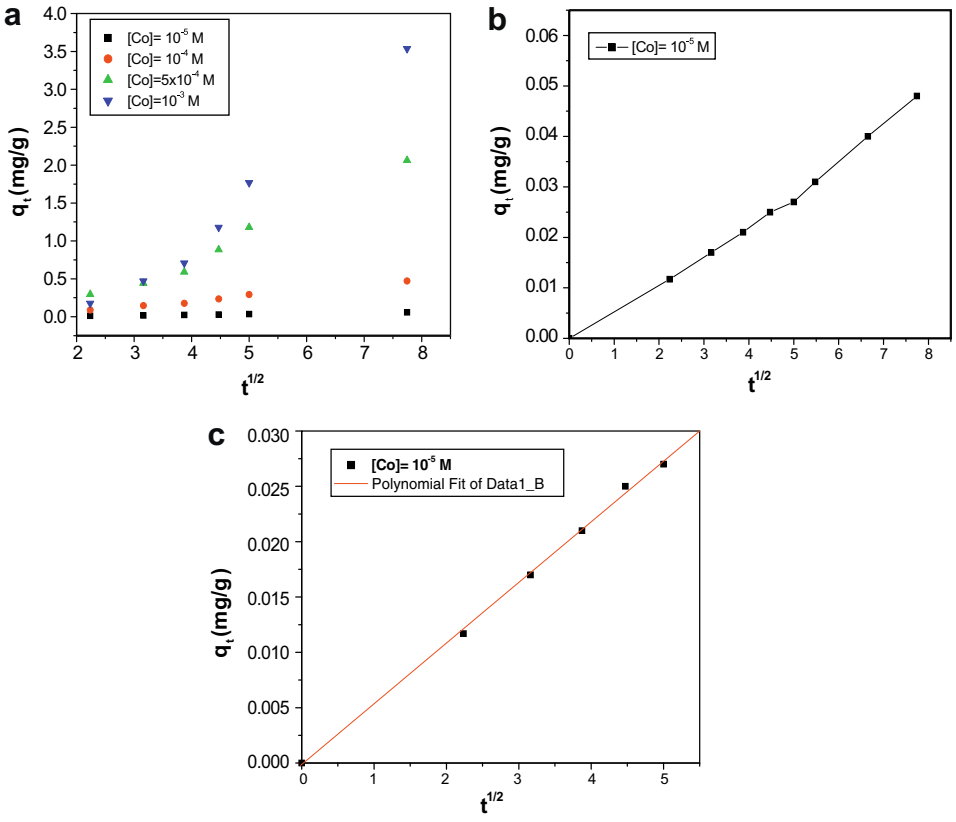

Fig. 10. Morris–Weber isotherm for Co(II) adsorption on CTU (2B) at different ion concentration.

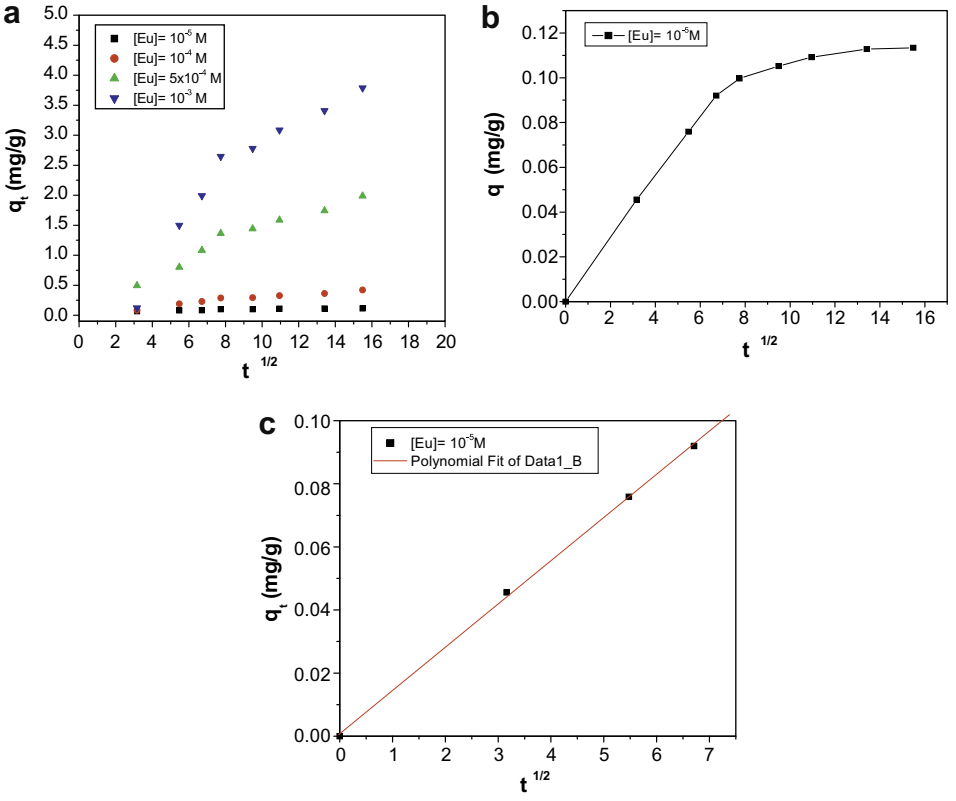

Fig. 11. Morris–Weber isotherm for Eu(III) adsorption on CTU (2B) at different ion concentration.

The kinetics of sorption of Co(II) and Eu(III) on CTU (2B) was also evaluated by the Morris–Weber isotherm model (Huh, Song, & Jeon, 2000):

$$q_t = k_d.t^{1/2} \quad (7)$$

where q_t is the concentration of the adsorbed ion (mg/g) at time t, and k_d is the rate constant for the intra-particle transport (mg/g $min^{1/2}$). According to this model, a plot of q_t versus t could predict the sorption mechanism of the studied ions. If a straight line (passing through the origin) is obtained, therefore, sorption of the ions onto the biopolymer follows a diffusion mechanism. In this case, the slope of the linear plot indicates the rate constant of the intra-particle transport (k_d). Morris–Weber relationship is represented in Figs. 10 and 11. From the reported data it is clear that Morris–Webber isotherm of the adsorption of Co(II) ions at 10^{-5} M ion concentration, fits well up to 25 min and then deviates. The slope of the linear plot obtained from the initial stage is shown in Fig. 10c. The calculated rate constant of the intra-particle transport of Co(II) at 10^{-5} M ion concentration is k_d = Slope = 0.00549 (mg/g $min^{-1/2}$), R^2 = 0.99861 All Morris–Webber relations plotted in Fig. 10a give a clear deviation after 20 min especially at 4×10^{-4} and 10^{-3} M ion concentration.

Morris–Webber isotherm of the adsorption of Eu(III) ions at 10^{-5} M ion concentration fits good up to 45 min and then deviates up to 240 min of contact time as shown in Fig. 11a. The slope of the linear plot obtained from the initial stage is shown in Fig. 11c. The calculated rate constant of the intra-particle transport of Eu(III) at 10^{-5} M ion concentration, is K_d = Slope = 0.01371 (mg/g $min^{-1/2}$), R^2 = 0.99932. All the plots in Fig. 11b gives a clear deviation after 45 min especially at 4×10^{-4} M and 10^{-3} M ion concentration.

4. Conclusion

This study indicates that CTU biopolymer is very effective for the adsorption of ^{60}Co and $^{153+154}$Eu radionuclides from aqueous solutions. It refers also to the ability of removing these radionuclides as divalent and trivalent cations from aqueous wastes and forming chelate complex with the chitosan chain. Freundlish and Langmuir isotherms best fit the adsorption data of chitosan with Co(II) and Eu(III) ions. The maximum adsorption capacity of the monolayer for Co(II) and Eu(III) were 29.47 (mg/g) and 34.54 (mg/g), respectively. Lagergren isotherm model is applied successfully to the resulting data, whereas Morris–Webber isotherm model does not fit for the entire time range of contact for Co(II) and Eu(IIII) adsorption. The change in the adsorbed ion concentration has a low a effect on the isotherm parameters values.

References

Abdou, S. E., Nagy, K. S. A., & Elsabee, M. Z. (2008). Extraction and characterization of chitin and chitosan from local sources. *Bioresource Technology, 99*, 1359.

Babel, S., & Kurniawan, T. A. (2003). Low-cost adsorbents for heavy metals uptake from contaminated water: A review. *Journal of Hazardous Materials B, 97*, 219.

Benavente, M., Arévalo, M., & Martínez, J. (2006). Speciation and Removal of Arsenic in column packed with chitosan. *Water Practice & Technology, 1*(4).

Blazquez, I., Vicente, F., Gallo, B., Ortiz, I., & Irabien, A. (1987). Application of chitosan to cobalt recovery: Evaluation by factorial design of experiments. *Journal of Applied Polymer Science, 33*, 2107.

Cardenas, G., Orlando, P., & Edelio, T. (2001). Synthesis and applications of chitosan mercaptanes as heavy metal retention agent. *International Journal of Biological Macromolecules, 28*, 167.

Chen, S. P., Wu, G. Z., & Zeng, H. Y. (2005). Preparation of high antimicrobial activity thiourea chitosan–Ag^+ complex. *Carbohydrate Polymers, 60*, 33.

Chu, K. H. (2002). Removal of copper from aqueous solution by chitosan in prawn shell: Adsorption equilibrium and kinetics. *Journal of Hazardous, Materials B, 90*, 77.

Evans, J. R., Davids, W. G., MacRae, J. D., & Amirbahman, A. (2002). Kinetics of cadmium uptake by chitosan-based crab shells. *Water Research, 36*, 3219.

Eweis, M., Elkholy, S. S., & Elsabee, M. Z. (2006). Antifungal efficacy of chitosan and its thiourea derivatives upon the growth of some sugar-beet pathogens. *International Journal of Biological Macromolecules, 38*, 1–8.

Guibal, E. (2004). Interactions of metal ions with chitosan-based sorbents: A review. *Separation and Purification Technology, 38*, 43.

Guibal, E., Vincent, T., & Mendoza, R. N. (2000). Synthesis and characterization of a thiourea derivative of chitosan for platinum recovery. *Journal of Applied Polymer Science, 75*, 119.

Huh, J. I., Song, D. I., & Jeon, Y. W. (2000). Sorption of phenol and alkylphenols from aqueous solution onto organically modified montmorillonite and applications of dual-mode sorption model. *Separation Science and Technology, 35*, 243.

Igwe, J. C., Ogunewe, D. N., & Abia, A. A. (2005). Competitive adsorption of Zn (II), Cd (II) AND Pb (II) ions from aqueous and non- aqueous solution by maize cob and husk. *African Journal of Biotechnology, 4*, 1113.

Juang, R. S., & Shao, H. J. (2002). A simplified equilibrium model for sorption of heavy metal ions from aqueous solutions on chitosan. *Water Research, 36*, 2999.

Justi, K. C., Fávere, V. T., Laranjeira, M. C. M., Neves, A., & Peralta, R. A. (2005). Kinetics and equilibrium adsorption of Cu(II), Cd(II), and Ni(II) ions by chitosan functionalized with 2[-bis-(pyridylmethyl)aminomethyl]-4-methyl-6-formylphenol. *Journal of Colloid and Interface Science, 291*, 369.

Khanal, D. R., Okamoto, Y., Miyatake, K., Shinobu, T., Shigemasa, Y., Tokura, S., et al. (2001). Protective effects of phosphated chitin (P-chitin) in a mice model of acute respiratory distress syndrome (ARDS). *Carbohydrate Polymers, 44*, 99.

Knaul, J. Z., Kasaai, M. R., Tambui, V., & Creber, K. A. M. (1998). Characterization of deacetylated chitosan and chitosan molecular weight review. *Canadian Journal of Chemistry, 76*, 1699.

Kumar, M. N. V. R., Muzzarelli, R. A. A., Muzzarelli, C., Sashiwa, H., & Domb, A. J. (2004). Chitosan chemistry and pharmaceutical perspectives. *Chemical Review, 104*, 6017.

Kurita, K., Mori, S., Nixhiyama, Y., & Harata, M. (2002). *N*-Alkylation of chitin and some characteristics of the novel derivatives. *Polymer Bulletin, 48*, 159.

McCarthy, M., Pratum, T., Hedges, J., & Benner, R. (1997). Chemical composition of dissolved organic nitrogen in the ocean. *Nature, 390*, 150.

Metwally, E. (2006). Kinetic studies for sorption of some metal ions from aqueous acid solutions onto TDA impregnated resin. *Journal of Radioanalytical and Nuclear Chemistry, 270*(3), 559.

Minamisawa, H., Jigiri, K., Arai, N., Okutani, T. (1996). Proceedings of the 45th Annual Meeting of the Japan Society for Analytical Chemistry, Sendai, September 95.

Minamisawa, H., Iwanamia, H., Arai, N., & Okutani, T. (1999). Adsorption behavior of cobalt(II) on chitosan and its determination by tungsten metal furnace atomic absorption spectrometry. *Analytica Chimica Acta, 378*, 279.

Minamisawa, M., Minamisawa, H., Yoshida, S., & Takai, N. (2004). *Journal of Agricultural Food Chemistry, 52*(18), 5606.

Mitani, T., Moriyama, A., & Ishi, H. (1992). Heavy metal uptake by swollen chitosan beads. *Bioscience Biotechnology and Biochemistry, 56*, 985.

Muzzarelli, R. A. A. (1973). *Natural chelating polymers* (1st ed.). Oxford: Pergamon Press.

Muzzarelli, R. R. A., Raith, G., & Tubertini, O. (1970). Separations of trace elements from sea water, brine and sodium and magnesium salt solutions by chromatography on chitosan. *Journal of Chromatography, 47*, 414.

Muzzarelli, R. R. A., & Rocchetti, R. (1974). The determination of vanadium in sea water by hot graphite atomic absorption spectrometry on chitosan after separation from salt. *Analalytica Chimica Acta, 70*, 283.

Muzzarelli, R. R. A., & Sipos, L. (1971). Chitosan for the collection from seawater of naturally occurring zinc, cadmium, lead and copper. *Talanta, 18*, 853.

Nishimura, Y., Imai, K., & Watari, K. (1995). *Chitin and Chitosan Research, 1*, 203.

Onsoyen, E., & Skaugrad, O. (1990). Metal recovery using chitosan. *Journal Chemical Technology and Biotechnology, 49*, 395.

Peter, M. G. (1995). *Journal of Macromolecular Science-Pure and Applied Chemistry, 4*, 629.

Ramnani, S. P., & Sabharwal, S. (2006). Adsorption behavior of Cr(VI) onto radiation crosslinked chitosan and its possible application for the treatment of wastewater containing Cr(VI). *Reactive and Functional Polymers, 66*(9), 902.

Ravindran, V., Steven, M. R., Badriyha, B. N., & Pirbazari, M. (1999). Modeling the sorption of toxic metals on chelant-impregnated adsorbent. *AIChE Journal, 45*(5), 1135.

Rhazi, M., Desbrières, J., Tolaimate, A., Rinaudo, M., Vottero, P., Alagui, A., et al. (2002). Influence of the nature of the metal ions on the complexation with chitosan; application to the treatment of liquid waste. *European Polymer Journal, 38*, 1523.

Rojas, G., Silva, J., Flores, J. A., Rodriguez, A., Lyc, M., & Maldonado, H. (2005). Adsorption of chromium onto cross-linked chitosan. *Separation and Purification Technology, 44*, 31.

Sakaguchi, T., Horikoshi, T., & Nakajima, A. (1981). Adsorption of Uranium by chitin and chitosan phosphate. *Agricultural and Biological Chemistry, 45*, 2191.

Schmuhl, R., Krieg, H. M., & Keizer, K. (2001). Adsorption of Cu(II) and Cr(VI) ions by chitosan: Kinetics and equilibrium studies. *Water SA, 27*(1), 1–8.

Sheha, R. R., & Metwally, E. (2007). Equilibrium isotherm modeling of cesium adsorption onto magnetic materials. *Journal of Hazardous Material, 143*, 354–361.

Silverstein, R. M., Webster, F. X., & Kiembe, D. J. (2005). *Spectrometric identification of organic compounds* (7th ed.). John Wiley and Sons, Inc.. p. 106.

Su, H., Wang, Z., & Tan, T. (2003). Adsorption of Ni^{2+} on the surface of molecularly imprinted adsorbent from *Penicillium chysogenum* mycelium. *Biotechnology Letters, 25*, 949.

Subhash, C. B., & Natarajan, R. (2000). A magnetic study of an fe-chitosan complex and its relevance to other biomolecules. *Biomacromolecules, 1*, 413.

Wan Ngah, W. S., Kamari, A., Fatinathan, S., & Ng, P. W. (2006). Adsorption of chromium from aqueous solution using chitosan beads. *Adsorption, 12*, 249.

Wang, Y., Kao, S., & Hsieh, H. (2003). A chemical surface modification of chitosan by glycoconjugates to enhance the cell-biomaterial interaction. *Biomacromolecules, 4*, 224.

Wu, F. C., Tsengm, R. L., & Juang, R. S. (2000). Comparative adsorption of metal and dye on flake- and bead-types of chitosan prepared from fishery wastes. *Journal of Hazardous Materials B, 73*, 63.